Universal Signature from Integrability to Chaos in Dissipative Open Quantum Systems

Gernot Akemann[*]
Faculty of Physics, Bielefeld University, Postfach 100131, 33501 Bielefeld, Germany
and Department of Mathematics, Royal Institute of Technology (KTH),
Brinellvägen 8, 114 28 Stockholm, Sweden

Mario Kieburg[†]
School of Mathematics and Statistics, University of Melbourne,
813 Swanston Street, Parkville, Melbourne, Victoria 3010, Australia

Adam Mielke[‡]
Faculty of Physics, Bielefeld University, Postfach 100131, 33501 Bielefeld, Germany

Tomaž Prosen[§]
Physics Department, Faculty of Mathematics and Physics, University of Ljubljana, Ljubljana 1000, Slovenia

(Received 15 October 2019; published 18 December 2019)

We study the transition between integrable and chaotic behavior in dissipative open quantum systems, exemplified by a boundary driven quantum spin chain. The repulsion between the complex eigenvalues of the corresponding Liouville operator in radial distance s is used as a universal measure. The corresponding level spacing distribution is well fitted by that of a static two-dimensional Coulomb gas with harmonic potential at inverse temperature $\beta \in [0, 2]$. Here, $\beta = 0$ yields the two-dimensional Poisson distribution, matching the integrable limit of the system, and $\beta = 2$ equals the distribution obtained from the complex Ginibre ensemble, describing the fully chaotic limit. Our findings generalize the results of Grobe, Haake, and Sommers, who derived a universal cubic level repulsion for small spacings s. We collect mathematical evidence for the universality of the full level spacing distribution in the fully chaotic limit at $\beta = 2$. It holds for all three Ginibre ensembles of random matrices with independent real, complex, or quaternion matrix elements.

DOI: 10.1103/PhysRevLett.123.254101

Introduction.—It has been a long discussed question how classically integrable and chaotic behavior carries over to the quantized world. A simple spectral measure was found in the spacing between neighboring eigenvalues of the corresponding Hamiltonian H. For closed systems it is Hermitian, $H = H^\dagger$, with real eigenvalues. Berry and Tabor conjectured [1] for quantum integrable systems to generically follow the one-dimensional (1D) Poisson distribution $p_P^{(1D)}(s) = e^{-s}$. In contrast, Bohigas, Giannoni, and Schmit (BGS) conjectured [2] (see Ref. [3]) chaotic systems [4] to follow random matrix theory (RMT) statistics in the corresponding symmetry class. Initially Dyson [5] had offered a first classification within RMT, distinguishing systems without or with time reversal at (half-)integer spin which is the celebrated "threefold way." Much evidence has been given to support this spectral classification in quantum systems, including neutron scattering, quantum billiards [2], and the hydrogen atom in a magnetic field [6], to name a few; see Refs. [7,8] for standard references. Starting from Berry's diagonal approximation [9] the BGS conjecture is now well understood from a semiclassical expansion [10,11].

Non-Hermitian operators play an equally important role in physics, e.g., in disordered systems [12] or quantum chromodynamics (QCD) with chemical potential [13]. Shortly after BGS, the above spectral distinction between integrable and chaotic was extended by Grobe, Haake, and Sommers (GHS) [14] to Markovian dissipative open quantum systems. These follow a Lindblad master equation,

$$\frac{d\rho}{dt}(t) = L\rho(t), \tag{1}$$

with L being the Liouville and ρ the density operator; see Ref. [15]. Postponing a detailed discussion for our example of a quantum XXZ spin chain—see Refs. [16,17]—the eigenvalues of L are real or come in complex conjugate pairs and can be used to characterize integrable or chaotic behavior; see below. Indeed this has been observed in many examples: for dissipative chaotic systems [18], the QCD Dirac operator [19], the adjacency matrix of directed graphs [20], and hardcore bosons with asymmetric hopping on a one-dimensional lattice at weak disorder [21]. In Ref. [14] GHS studied periodically kicked tops with damping and the corresponding discrete quantum map. In the integrable limit they found agreement between the nearest neighbor spacing in radial distance s of its complex bulk eigenvalues and the two-dimensional (2D) Poisson distribution

$$p_P^{(2D)}(s) = \frac{\pi}{2} s e^{-\pi s^2/4}, \tag{2}$$

which are local quantities. In the fully chaotic limit the spacing distribution agrees with the corresponding distribution of the Ginibre ensemble [22] of complex Gaussian non-Hermitian random matrices (GinUE), given by Ref. [14],

$$p_{\rm GinUE}(s) = \left(\prod_{k=1}^{\infty} \frac{\Gamma(1+k, s^2)}{k!}\right) \sum_{j=1}^{\infty} \frac{2 s^{2j+1} e^{-s^2}}{\Gamma(1+j, s^2)}, \tag{3}$$

with $\Gamma(1+k, s^2) = \int_{s^2}^{\infty} t^k e^{-t} dt$ being the incomplete Γ function. GHS conjectured that the local spectrum of a generic chaotic dissipative open quantum system in the bulk should follow the same statistics. This was somewhat surprising, as they showed that the complex Ginibre ensemble leading to Eq. (3) does not satisfy the global symmetries of dissipative open quantum systems [14], unlike its real counterpart. Grobe and Haake showed in Ref. [23] that, based on these symmetries, using perturbative arguments for small distance s, the repulsion is universally cubic. This repulsion is shared by the complex Ginibre ensemble (3), as well as by a larger class of complex normal random matrices [24]. The global statistics of Lindblad operators has also been compared to random matrices; see Refs. [25–28].

Our goals are, first, to provide a further example for the GHS conjecture for complex spectra of integrable or quantum chaotic systems to be true, given by boundary driven quantum spin chains. These are many-body systems with no meaningful semiclassical limit, so the term *quantum chaos* is understood as the absence of integrability or weak coupling thereof, while its rigorous definition is still lacking. Second, we will show that in the intermediate regime the full spacing distribution is very well described by a static 2D Coulomb gas at inverse temperature $\beta \in (0, 2]$ in a harmonic potential. Its joint distribution of the set z of N point charges at rescaled positions $\sqrt{2/\beta} z_{i=1,\ldots,N} \in \mathbb{C}$ [29] reads [30]

$$\mathcal{P}_\beta(z) \propto \exp\left(-\sum_{i=1}^{N} |z_i|^2 + \frac{\beta}{2} \sum_{i\neq j}^{N} \ln|z_i - z_j|\right). \tag{4}$$

For $\beta = 0$ this leads to the Poisson distribution (2) [18], whereas $\beta = 2$ corresponds to the level spacing distribution (3) [14]. Third, we collect mathematical evidence for the fully chaotic case (3) at $\beta = 2$ to be universal in the bulk of the spectrum, regardless of the constraints [14]. With bulk we mean to stay macroscopically away from any edge or critical points (here, the real line) of the spectrum. This universality holds for the complex, real [31], and quaternion Ginibre ensemble—to be presented here—and for non-Gaussian extensions [32] of the two former ones. This is in contrast to random matrices with real spectra, where quantum chaotic behavior is distinct for the three Dyson classes, corresponding to a 1D log gas at different values $\beta = 1, 2, 4$. For complex bulk eigenvalues of chaotic systems, the possibility of distinguishing their global symmetry is thus lost. To prepare our 2D data from the Liouville operator L for a comparison, we need to unfold the complex spectrum. While this is straightforward for real spectra [8], we discuss the literature [19] and present our method below.

Integrable and nonintegrable quantum spin chains.— The system we consider is a Heisenberg XXZ Hamiltonian H of N spins $1/2$, comprising nearest and next-to-nearest neighbor interactions,

$$H = J \sum_{l=1}^{N-1} (\sigma_l^x \sigma_{l+1}^x + \sigma_l^y \sigma_{l+1}^y + \Delta \sigma_l^z \sigma_{l+1}^z) + J' \sum_{l=1}^{N-2} (\sigma_l^x \sigma_{l+2}^x + \sigma_l^y \sigma_{l+2}^y + \Delta' \sigma_l^z \sigma_{l+2}^z), \tag{5}$$

with $J, J', \Delta, \Delta' \in \mathbb{R}$. We denote the three Pauli matrices by σ_l^α, $\alpha = x, y, z$, for each single spin $l = 1, \ldots, N$. With each spin a dephasing operator

$$L_l = \sqrt{\gamma} \sigma_l^z, \quad l = 1, \ldots, N \quad \text{and} \quad \gamma > 0 \tag{6}$$

is associated. Additionally, we introduce dissipation of polarization at the two ends of the spin chain via the Lindblad operators

$$L_{-1} = \sqrt{\gamma_L^+} \sigma_1^+, \qquad L_0 = \sqrt{\gamma_L^-} \sigma_1^-, \qquad L_{N+1} = \sqrt{\gamma_R^+} \sigma_N^+, \qquad L_{N+2} = \sqrt{\gamma_R^-} \sigma_N^-, \tag{7}$$

where $\gamma_L^\pm, \gamma_R^\pm > 0$ and $\sigma_l^\pm = \sigma_l^x \pm i \sigma_l^y$. The Liouville operator L acting on a density operator ρ in the master equation (1) is given by [16,17]

$$L\rho = -i[H, \rho] + \sum_{l=-1}^{N+2} (2 L_l \rho L_l^\dagger - \{L_l^\dagger L_l, \rho\}). \tag{8}$$

The commutator and anticommutator are denoted by $[\cdot,\cdot]$ and $\{\cdot,\cdot\}$, respectively; see Ref. [15].

What we are interested in is the spectral statistics of the Liouville operator L considered as a $(4^N - 1) \times (4^N - 1)$ real matrix, acting on the vector space of density operators. The reduction in dimension by 1 results from the fixed trace condition on ρ and is represented by the identity matrix.

The operator L is real because $\rho \to L\rho$ preserves the Hermiticity. The statistics of L should indicate whether the Lindblad master equation (1) behaves in an integrable or chaotic way. For this purpose we recall some properties of the operator L in our example.

Switching off all incoherent processes $\gamma = \gamma_L^\pm = \gamma_R^\pm = 0$, the operator L becomes a real antisymmetric (because of $\mathrm{Tr}\rho_1[H,\rho_2] = -\mathrm{Tr}[H,\rho_1]\rho_2$) and chiral (due to $[H,\rho]^T = -[H,\rho^T]$) matrix so that the spectrum becomes 1D and is purely imaginary and symmetric about the origin. When also suppressing the next-to-nearest neighbor interactions ($J' = 0$), the spectrum is completely integrable. With increasing $J' \neq 0$ chaotic behavior will take over, and Wigner's $\beta = 1$ statistics in the bulk of the spectrum applies; see Ref. [33] for a review of the standard 1D RMT analysis of this setup.

The situation changes drastically when the dissipative processes are switched on (γ, $\gamma_L^\pm$, $\gamma_R^\pm \neq 0$). Then, the Liouville operator L becomes a real nonsymmetric matrix, and its eigenvalues spread into the complex plane. Nonetheless, there is still a good quantum number which has to be taken into account—namely, the total spin polarization $S = \sum_{l=1}^N \sigma_l^z$. It keeps the coherent processes invariant due to $[H,S] = 0$, while all additional incoherent dissipative processes result in the following weak symmetry of the Liouvillian [17],

$$[L(\rho), S] = L([\rho, S]), \tag{9}$$

which is equivalent to the vanishing commutator of the matrix representations of L and $[S,\cdot]$.

Let $|s,n\rangle$ be an eigenstate of H with $S|s,n\rangle = s|s,n\rangle$, and let $s = -N/2, -(N-2)/2, \ldots, N/2$. Then, the eigenvalue equation of the state $|s,n\rangle\langle s',n'|$ under the adjoint action of S is

$$[S, |s,n\rangle\langle s',n'|] = (s-s')|s,n\rangle\langle s',n'|. \tag{10}$$

Defining $M = N - s + s' \in \{0,1,\ldots,2N\}$, the dimension κ of the eigenspace of the fixed quantum number $s - s' = N - M$ is given by $\kappa = \binom{2N}{M} - \delta_{NM}$, where the Kronecker delta represents the identity matrix which obviously belongs to the $M = N$ state space. Therefore, L decomposes into block matrices, and one needs to study the spectral statistics of each of these matrices separately. Since we are interested in a good statistical error, it is favorable to choose M close to N, as then the number of eigenvalues $\kappa \sim 2^{2N}/N$ grows exponentially quickly for large N.

Comparing data with predictions.—We have generated four realizations of the Liouville operator (8) where, for all four cases, $N = 10$ and $M = 7$, and we set the scale to $J = 1$. Thus, we have had in total 77 520 eigenvalues per case to analyze.

(a) The boundary driven XX chain ($\Delta = 0$) with bulk dephasing. The parameters are chosen as $J' = 0$, $\gamma_L^+ = 0.5$, $\gamma_L^- = 1.2$, $\gamma_R^+ = \gamma = 1$, and $\gamma_R^- = 0.8$. The model is equivalent to the Fermi-Hubbard chain with imaginary interaction $U = i\gamma$ with off-diagonal boundaries—see Ref. [34]—which is known to be Bethe ansatz integrable. According to the GHS conjecture, we expect Poisson statistics for the Liouvillian spectrum; see Fig. 1(a).

(b) The isotropic Heisenberg XXX chain ($\Delta = 1$) with pure-source and pure-sink driving. The parameters are $J' = 0$, $\gamma_L^+ = 0.6$, $\gamma_R^- = 1.4$, $\gamma_L^- = \gamma_R^+ = \gamma = 0$ in this regime. The steady state (zero mode) of this problem is known to be exactly solvable [16]; however, the full Liouvillian spectrum shows nonintegrable behavior [see Fig. 1(b)].

(c) The XXX chain ($\Delta = 1$) with arbitrary polarizing boundary driving. Here, we chose the parameters $J' = 0$, $\gamma_L^+ = 0.5$, $\gamma_L^- = 0.3$, $\gamma_R^+ = 0.3$, $\gamma_R^- = 0.9$, and $\gamma = 0$. The bulk Hamiltonian of this model is well known to be integrable via the Bethe ansatz, but with the boundary driving not even the steady state seems to be exactly solvable. The spectrum in Fig. 1(c) confirms that its dynamics is fully chaotic, according to the GHS conjecture.

(d) The XXZ chain with nearest neighbor and next-to-nearest neighbor interactions. We have chosen $J' = 1$, $\Delta = 0.5$, and $\Delta' = 1.5$ with the same dephasing parameters as in (c). This time, even the bulk Hamiltonian is nonintegrable (quantum chaotic), so we expect Ginibre statistics following the GHS conjecture, which is confirmed in Fig. 1(d).

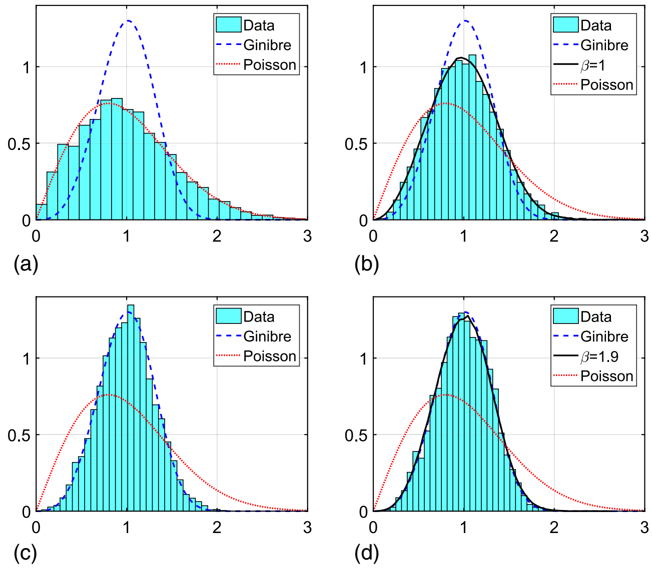

FIG. 1. Comparison of the level spacing distributions for various Liouville operators (8), the analytical spacing distributions (2) (Poisson $\beta = 0$, dotted line) and (3) (Ginibre $\beta = 2$, dashed line) as well as fits to general Coulomb gas (4) simulations [(b) and (d), solid lines]. Unfolding (13) is used with the smearing parameter $\sigma = 4.5\bar{s}$ [see Eq. (13)], where the mean spacing varies from $\bar{s} = 0.0036$ to 0.0045 for the datasets (a)–(d). The first moment of all spacings is normalized to unity.

All four datasets are depicted in Fig. 1, illustrating the integrable [Fig. 1(a)], intermediate [Fig. 1(b)], and apparently fully chaotic cases [Figs. 1(c) and 1(d)]. Note that the intermediate case [Fig. 1(b)] flows closer (and is expected to converge) to fully chaotic statistics by increasing the dimension κ. We compare this with the 2D Poisson distribution (2), the distribution of the numerically generated Coulomb gas (4) with the best fit for β, and the level spacing distribution (3) of the complex Ginibre ensemble. The Kolmogorov-Smirnov distances [35] between the empirical distributions of the spectrum of L, and each of these curves (after fitting β) are listed in Table I. The spacings for the Coulomb gas are obtained by generating points with the distribution (4) by using the Metropolis algorithm, following Ref. [36], and then determining the spacing numerically. Figure 1 confirms our expectations of an extended GHS conjecture [14,23] for dissipative open quantum systems to hold, even without classically chaotic correspondents.

Unfolding of complex spectra.—In order to compare the spectrum of L with the spectral statistics of the 2D Coulomb gas (2)–(4), we need to unfold the spectrum. This means that we have to separate the fluctuations (fl), which are supposedly universal, from the global, averaged (av) spectral density, which is system specific:

$$\rho(x,y) = \sum_{i=1}^{N} \delta^{(2)}(z - z_i) = \rho_{\text{av}}(x,y) + \rho_{\text{fl}}(x,y), \quad (11)$$

where $z = x + iy$. For real spectra unfolding is achieved by introducing the cumulative spectral function and fitting the smooth part $\eta(x) = \int_{-\infty}^{x} \rho_{\text{av}}(t)dt$ [8]. For complex spectra this is more involved. Following Ref. [19], unfolding is a map

$$z \to z' = x' + iy' = u(x,y) + iv(x,y), \quad (12)$$

to be found, that satisfies certain conditions. First, after unfolding the density has to be unity (or constant), $\rho_{\text{av}}(x',y') = 1$, or in other words the Jacobian of the transformation (12) has to cancel the density before unfolding, $dx'dy' = \rho_{\text{av}}(x,y)dxdy$. This is certainly not unique, and we believe that, second, local isotropy has to be achieved, e.g., using conformal maps [19]. Following the symmetry of their data, Markum *et al.* [19] proposed unfolding in strips parallel to the x axis, in choosing $y' = y$ and thus $x' = \int_{-\infty}^{x} \rho_{\text{av}}(t,y)dt = u(x,y)$. Apparently for more general datasets this choice is not ideal, e.g., for products of M Ginibre matrices where the density at the origin is singular [37]. Its local statistics is known to still follow the complex Ginibre ensemble [38], making proper unfolding crucial.

In fact we found a much simpler method following Eq. (11) by approximating $\rho_{\text{av}}(x,y)$ by a sum of Gaussian distributions around each eigenvalue z_j,

$$\rho_{\text{av}}(x,y) \approx \frac{1}{2\pi\sigma^2 N} \sum_{j=1}^{N} \exp\left(-\frac{1}{2\sigma^2}|z - z_j|^2\right). \quad (13)$$

The measured spacing at a point z_0 is then simply multiplied by $\sqrt{\rho_{\text{av}}(x_0,y_0)}$. Testing this on spectra of the products of random matrices, the choice $\sigma = 4.5\bar{s}$ in terms of the global mean spacing $\bar{s}$ leads to very good results; see Ref. [39]. This method is applied to our datasets in Figs. 1(a)–(d).

TABLE I. The Kolmogorov distance between the empirical data shown in Fig. 1, the Poisson distribution (2), the fitted value for β (specified in the inset) of the Coulomb gas, and the Ginibre spacing distribution (3).

System	Poisson	Fitted Coulomb β	Ginibre
(a)	0.015	⋯	0.15
(b)	0.10	0.0092 ($\beta = 1$)	0.058
(c)	0.15	⋯	0.012
(d)	0.16	0.0094 ($\beta = 1.9$)	0.012

Random matrix universality.—The question raised by the conjecture of GHS was why the fully chaotic case should be compared with the predictions of the complex Ginibre ensemble. Grobe *et al.* [14] showed that, due to Hermiticity constraints, generic dissipative open quantum systems lead to a spectrum of real and complex conjugate eigenvalue pairs. Thus, one would expect the real or quaternion Ginibre ensemble (GinOE or GinSE) sharing this property to apply, and not the GinUE. However, Grobe *et al.* found an agreement of their data from periodically kicked tops with damping with the GinUE—results for the GinOE or GinSE were not available at the time.

While the results for the GinSE became available soon after the publication of Ref. [42], including the spacing distribution at the origin [which is different from the GinUE (3)], the GinOE was independently solved much later by three groups [31,43,44]. They are given by so-called Pfaffian point processes, with matrix valued kernels as the main building block.

Once all density correlation functions are known, all spectral information is given, including the spacing. While close to the real line all three ensembles differ, it was shown that at the edge of the spectrum the GinSE [45] and GinOE [31] agree with the GinUE [46]. It is therefore natural to ask whether or not this agreement continues to hold in the bulk. For the GinOE this was answered affirmatively in Ref. [31], and in the Supplemental Material [39] we show that this also holds for the GinSE. Below we give a heuristic argument (see also Ref. [11]) for why all three symmetry classes yield the same spacing distribution in the bulk, and it is thus universal.

The joint probability density function (jpdf) of eigenvalues for all three Ginibre ensembles read [22,47]

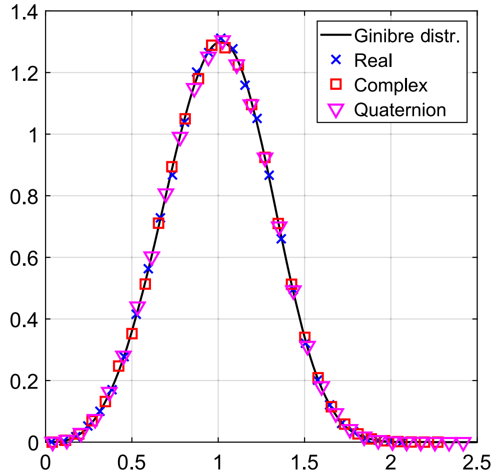

FIG. 2. Comparison of the spacing distribution (3) with normalized first moment and those of the GinOE (blue crosses), GinUE (red squares), and GinSE (purple triangles) in the bulk of the spectrum. For the latter we use the standard $2N$-dimensional representation of an N-dimensional quaternionic matrix, making the complex eigenvalues unique; see Ref. [22]. An ensemble of 1000 500×500 matrices has been generated in a Monte Carlo simulation. Here, the unfolding is trivial due to a uniform density of all three ensembles.

$$\mathcal{P}^{(k)}_{\mathrm{GinOE}}(z)\propto|\Delta_M(z)|^2\Delta_k(x)\prod_{i,j=1}^{M}(z_i-z_j^*)\prod_{i=1}^{k}\prod_{j=1}^{M}|z_j-x_i|^2 \times\prod_{l=1}^{k}e^{-(1/2)x_l^2}\prod_{j=1}^{M}\mathrm{sgn}[\mathrm{Im}(z_j)]\mathrm{erfc}[\sqrt{2}\mathrm{Im}(z_j)] \times e^{-(1/2)(z_j^2+z_j^{*2})},$$

$$\mathcal{P}_{\mathrm{GinUE}}(z)\propto|\Delta_N(z)|^2\prod_{j=1}^{N}e^{-|z_j|^2},$$

$$\mathcal{P}_{\mathrm{GinSE}}(z)\propto|\Delta_M(z)|^2\prod_{i>j}^{M}|z_i-z_j^*|^2\prod_{j=1}^{M}|z_j-z_j^*|^2e^{-|z_j|^2}. \quad (14)$$

Here, $\Delta_N(a)=\prod_{j>k}^{N}(a_j-a_k)$ denotes the Vandermonde determinant and erfc the complementary error function. The $N=k+2M$ eigenvalues in the GinOE are ordered to yield a positive density, and k counts the number of real eigenvalues; see, e.g., Refs. [31,43,44] for details, and for the GinSE $N=2M$.

For large N there are only $k\propto\sqrt{N}$ real eigenvalues x_l on average [48], and thus we consider $M\sim N/2$. Raising the Vandermonde to the exponent leads to the Coulomb gas picture (4) at $\beta=2$ for the GinUE. Notice that the other two ensembles are *not* proportional to $|\Delta_N(z)|^\beta$ for $\beta=1$, 4. The limiting spectral density is constant on a disk of radius $\mathcal{O}(\sqrt{N})$ for all three Ginibre ensembles, and also for Coulomb gases (4) for all $\beta>0$; see, e.g., Ref. [49] for a review. The local bulk statistics is defined by zooming into the vicinity of radius $R=\mathcal{O}(1)$ of a few mean level spacings around a bulk eigenvalue z_0, chosen far away from the real axis and the edge of the support. Close to z_0, complex conjugate and real eigenvalues are of the order $\mathcal{O}(\sqrt{N})$ away from z_0 and thus do not contribute to the local spectral statistics. Hence all jpdf's (14) become locally proportional to

$$\sim\prod_{j:|z_j-z_0|<R}|z_j-z_0|^2 \quad (15)$$

for large N. Thus, all three ensembles coincide locally and share the GinUE spacing distribution (3). In Fig. 2, we illustrate this argument with Monte Carlo simulations of all three Ginibre ensembles in the bulk, finding perfect agreement. Very recently numerical evidence has been given for four further symmetry classes to follow the spacing (3) of the GinUE [50]. While Hamazaki *et al.* identified two ensembles where the spacing differs, it remains to be seen how many classes emerge in the bulk from the complete list of non-Hermitian ensembles [51–53].

Conclusions.—We have studied universal spectral properties of dissipative open quantum systems. Their corresponding Liouville operator L generically exhibits complex eigenvalue statistics. In our example we have numerically diagonalized boundary driven quantum spin chains of the XXZ type, with nearest and next-to-nearest neighbor interactions with different sets of couplings. Depending on these parameters, it is known that the system undergoes a transition from integrable to chaotic behavior. The spacing distribution in radial distance between the complex eigenvalues of L has been shown to be an efficient measure to observe this transition. Generalizing the conjecture of Grobe, Haake, and Sommers for the extreme cases, we have shown that the intermediate statistics is very well described by a two-dimensional Coulomb gas with harmonic potential by fitting to an inverse temperature $\beta\in[0,2]$. Furthermore, we have generalized the universality argument of these authors from a cubic repulsion for small spacing in the chaotic case $\beta=2$ to hold for the full distribution in all three Ginibre ensembles. Here, we have contributed analytically to the quaternion case and have illustrated this with numerical evidence.

Several open questions deserve further study. While for quantum systems with real eigenvalues the emergence of random matrix statistics in the chaotic regime is well understood, using a semiclassical expansion, such an approach is not developed here. Further examples for physical systems with complex eigenvalues should be studied throughout the transition region from integrable to chaotic behavior to see whether the description by a 2D Coulomb gas is indeed universal.

This work was partly funded by the Wallenberg foundation (G. A.), the German Science Foundation DFG within CRC1283, “Taming uncertainty and profiting from randomness and low regularity in analysis, stochastics, and their applications" (G. A. and M. K.), and within IRTG2235, "Searching for the regular in the irregular: Analysis of singular and random systems" (A. M.), by the European Research Council under Advanced Grant No. 694544—OMNES (T. P.), and by the Slovenian Research Agency (ARRS) under Program No. P1-0402 (T. P.). Support from the Simons Center for Geometry and Physics, Stony Brook University, where part of this work was completed (G. A. and M. K.), is gratefully acknowledged, as are the fruitful discussions with Maurice Duits (G. A.).

[*]akemann@physik.uni-bielefeld.de
[†]m.kieburg@unimelb.edu.au
[‡]amielke@math.uni-bielefeld.de
[§]tomaz.prosen@fmf.uni-lj.si

[1] M. V. Berry and M. Tabor, Proc. R. Soc. A **356**, 375 (1977).
[2] O. Bohigas, M. J. Giannoni, and C. Schmit, Phys. Rev. Lett. **52**, 1 (1984); J. Phys. Lett. (Paris) **45**, 1015 (1984).
[3] G. Casati, F. Valz-Gris, and I. Guarneri, Lett. Nuovo Cimento **28**, 279 (1980).
[4] P. Walters, *An Introduction to Ergodic Theory* (Springer, Heidelberg, 1982).
[5] F. J. Dyson, J. Math. Phys. (N.Y.) **3**, 1199 (1962).
[6] D. Wintgen and H. Friedrich, Phys. Rev. A **35**, 1464 (1987).
[7] H.-J. Stöckmann, *Quantum Chaos: An Introduction* (Cambridge University Press, Cambridge, England, 1999).
[8] T. Guhr, A. Müller-Groeling, and H. A. Weidenmüller, Phys. Rep. **299**, 189 (1998).
[9] M. V. Berry, Proc. R. Soc. A **400**, 229 (1985).
[10] M. Sieber and K. Richter, Phys. Scr. **T90**, 128 (2001).
[11] S. Müller, S. Heusler, A. Altland, P. Braun, and F. Haake, New J. Phys. **11**, 103025 (2009).
[12] N. Hatano and D. R. Nelson, Phys. Rev. Lett. **77**, 570 (1996).
[13] M. A. Stephanov, Phys. Rev. Lett. **76**, 4472 (1996).
[14] R. Grobe, F. Haake, and H.-J. Sommers, Phys. Rev. Lett. **61**, 1899 (1988).
[15] H.-P. Breuer and F. Petruccione, *The Theory of Open Quantum Systems* (Oxford University Press, Oxford, 2007).
[16] T. Prosen, Phys. Rev. Lett. **107**, 137201 (2011).
[17] B. Buča and T. Prosen, New J. Phys. **14**, 073007 (2012).
[18] F. Haake, *Quantum Signatures of Chaos*, 3rd ed. (Springer, Heidelberg, 2010).
[19] H. Markum, R. Pullirsch, and T. Wettig, Phys. Rev. Lett. **83**, 484 (1999).
[20] B. Ye, L. Qiu, X. Wang, and T. Guhr, Commun. Nonlinear Sci. Numer Simulat. **20**, 1026 (2015).
[21] R. Hamazaki, K. Kawabata, and M. Ueda, Phys. Rev. Lett. **123**, 090603 (2019).
[22] J. Ginibre, J. Math. Phys. (N.Y.) **6**, 440 (1965).
[23] R. Grobe and F. Haake, Phys. Rev. Lett. **62**, 2893 (1989).
[24] G. Oas, Phys. Rev. E **55**, 205 (1997).
[25] S. Denisov, T. Laptyeva, W. Tarnowski, D. Chruściński, and K. Życzkowski, Phys. Rev. Lett. **123**, 140403 (2019).
[26] T. Can, arXiv:1902.01442.
[27] T. Can, V. Oganesyan, D. Ograd, and S. Gopalakrishnan, arXiv:1902.01414.
[28] L. Sa, P. Ribeiro, and T. Prosen, arXiv:1905.02155.
[29] The rescaling is made for the limit $\beta \to 0$ to exist, leading to noninteracting particles confined by a Gaussian potential.
[30] P. J. Forrester, *Log-Gases and Random Matrices* (Princeton University Press, Princeton, NJ, 2010).
[31] A. Borodin and C. D. Sinclair, Commun. Math. Phys. **291**, 177 (2009).
[32] T. Tao and V. Vu, Ann. Probab. **43**, 782 (2015).
[33] L. D'Alessio, Y. Kafri, A. Polkovnikov, and M. Rigol, Adv. Phys. **65**, 239 (2016).
[34] M. V. Medvedyeva, F. H. L. Essler, and T. Prosen, Phys. Rev. Lett. **117**, 137202 (2016).
[35] R. R. Wilcox, *Introduction to Robust Estimation and Hypothesis Testing*, 2nd ed. (Elsevier, Amsterdam, 2005).
[36] D. Chafaï and G. Ferré, J. Stat. Phys. **174**, 692 (2019).
[37] Z. Burda, R. A. Janik, and B. Waclaw, Phys. Rev. E **81**, 041132 (2010).
[38] G. Akemann and Z. Burda, J. Phys. A **45**, 465201 (2012).
[39] See Supplemental Material at http://link.aps.org/supplemental/10.1103/PhysRevLett.123.254101, which includes Refs. [40,41], for where details including checks of our unfolding method as well as a mathematical proof for the bulk universality of the GinSE can be found.
[40] *NIST Handbook of Mathematical Functions*, edited by F. W. L Olver *et al.* (Cambridge University Press, Cambridge, England, 2010).
[41] E. Kanzieper, J. Phys. A **35**, 6631 (2002).
[42] M. L. Mehta, *Random Matrices*, 2nd ed. (Academic Press, New York, 1990).
[43] H.-J. Sommers, J. Phys. A **40**, F671 (2007).
[44] P. J. Forrester and T. Nagao, Phys. Rev. Lett. **99**, 050603 (2007).
[45] B. Rider, J. Phys. A **36**, 3401 (2003).
[46] P. J. Forrester and G. Honner, J. Phys. A **32**, 2961 (1999).
[47] N. Lehmann and H.-J. Sommers, Phys. Rev. Lett. **67**, 941 (1991).
[48] K. B. Efetov, Phys. Rev. Lett. **79**, 491 (1997).
[49] S. Serfaty, in *Random Matrices*, IAS/Park City Mathematics Series Vol. 26, edited by A. Borodin, I. Corwin, and A. Guionnet (AMS, Providence, 2019), p. 341–387.
[50] R. Hamazaki, K. Kawabata, N. Kura, and M. Ueda, arXiv:1904.13082.
[51] D. Bernard and A. LeClair, in *Statistical Field Theories* (Springer, Dordrecht, 2002), pp. 207–214.
[52] U. Magnea, J. Phys. A **41**, 045203 (2008).
[53] K. Kawabata, K. Shiozaki, M. Ueda, and M. Sato, Phys. Rev. X **9**, 041015 (2019).